OPEN ACCESS



DELVE 6: An Ancient, Ultra-faint Star Cluster on the Outskirts of the Magellanic Clouds

```
W. Cerny<sup>1</sup>, A. Drlica-Wagner<sup>2,3,4</sup>, T. S. Li<sup>5</sup>, A. B. Pace<sup>6</sup>, K. A. G. Olsen<sup>7</sup>, N. E. D. Noël<sup>8</sup>, R. P. van der Marel<sup>9,10</sup>, J. L. Carlin<sup>11</sup>, Y. Choi<sup>12</sup>, D. Erkal<sup>8</sup>, M. Geha<sup>1</sup>, D. J. James<sup>13,14</sup>, C. E. Martínez-Vázquez<sup>15</sup>, P. Massana<sup>16</sup>, G. E. Medina<sup>5</sup>, A. E. Miller<sup>17,18,19,20</sup>, B. Mutlu-Pakdil<sup>21</sup>, D. L. Nidever<sup>7,16</sup>, J. D. Sakowska<sup>8</sup>, G. S. Stringfellow<sup>22</sup>, J. A. Carballo-Bello<sup>23</sup>, P. S. Ferguson<sup>24</sup>, N. Kuropatkin<sup>2</sup>, S. Mau<sup>25,26</sup>, E. J. Tollerud<sup>9</sup>, and A. K. Vivas<sup>27</sup>
                                                                                           DELVE Collaboration
                                         <sup>1</sup> Department of Astronomy, Yale University, New Haven, CT 06520, USA; william.cerny@yale.edu
                                                        <sup>2</sup> Fermi National Accelerator Laboratory, P.O. Box 500, Batavia, IL 60510, USA
                                                <sup>3</sup> Kavli Institute for Cosmological Physics, University of Chicago, Chicago, IL 60637, USA
                                             <sup>4</sup> Department of Astronomy and Astrophysics, University of Chicago, Chicago, IL 60637, USA
                          <sup>5</sup> Department of Astronomy and Astrophysics, University of Toronto, 50 St. George Street, Toronto, ON M5S 3H4, Canada
                                 McWilliams Center for Cosmology, Carnegie Mellon University, 5000 Forbes Avenue, Pittsburgh, PA 15213, USA
                            NSF's National Optical-Infrared Astronomy Research Laboratory, 950 North Cherry Avenue, Tucson, AZ 85719, USA
                                                              Department of Physics, University of Surrey, Guildford GU2 7XH, UK
                                                  <sup>9</sup> Space Telescope Science Institute, 3700 San Martin Drive, Baltimore, MD 21218, USA
                     Center for Astrophysical Sciences, Department of Physics & Astronomy, Johns Hopkins University, Baltimore, MD 21218, USA

11 Rubin Observatory/AURA, 950 North Cherry Avenue, Tucson, AZ 85719, USA
                                               <sup>12</sup> Department of Astronomy, University of California, Berkeley, Berkeley, CA 94720, USA
                                                                   ASTRAVEO LLC, P.O. Box 1668, Gloucester, MA 01931, USA
                                                              ASTRAVEO ELC., 1.0. Box 1000, Gloucester, MA 01930, USA
Applied Materials Inc., 35 Dory Road, Gloucester, MA 01930, USA
                                                 <sup>15</sup> Gemini Observatory, NSF's NOIRLab, 670 North A'ohoku Place, Hilo, HI 96720, USA
                                       Department of Physics, Montana State University, P.O. Box 173840, Bozeman, MT 59717-3840, USA
                             <sup>17</sup> School of Mathematical and Physical Sciences, Macquarie University, Balaclava Road, Sydney, NSW 2109, Australia
               Research Centre for Astronomy, Astrophysics and Astrophotonics, Macquarie University, Balaclava Road, Sydney, NSW 2109, Australia

Leibniz-Institut für Astrophysik Potsdam (AIP), An der Sternwarte 16, D-14482 Potsdam, Germany

Institut für Physik und Astronomie, Universität Potsdam, Haus 28, Karl-Liebknecht-Str. 24/25, D-14476 Golm (Potsdam), Germany

Department of Physics and Astronomy, Dartmouth College, Hanover, NH 03755, USA
                              <sup>22</sup> Center for Astrophysics and Space Astronomy, University of Colorado, 389 UCB, Boulder, CO 80309-0389, USA
                        <sup>23</sup> Instituto de Alta Investigación, Sede Esmeralda, Universidad de Tarapacá, Av. Luis Emilio Recabarren 2477, Iquique, Chile
                                                     Department of Physics, University of Wisconsin-Madison, Madison, WI 53706, USA
                                             Department of Physics, Stanford University, 382 Via Pueblo Mall, Stanford, CA 94305, USA
                           <sup>26</sup> Kavli Institute for Particle Astrophysics & Cosmology, Stanford University, P.O. Box 2450, Stanford, CA 94305, USA
              <sup>27</sup> Cerro Tololo Inter-American Observatory, NSF's National Optical-Infrared Astronomy Research Laboratory, Casilla 603, La Serena, Chile
                                           Received 2023 June 7; revised 2023 August 4; accepted 2023 August 4; published 2023 August 18
```

Abstract

We present the discovery of DELVE 6, an ultra-faint stellar system identified in the second data release of the DECam Local Volume Exploration (DELVE) survey. Based on a maximum-likelihood fit to its structure and stellar population, we find that DELVE 6 is an old ($\tau > 9.8$ Gyr at 95% confidence) and metal-poor ([Fe/H] < -1.17 dex at 95% confidence) stellar system with an absolute magnitude of $M_V = -1.5^{+0.4}_{-0.6}$ mag and an azimuthally averaged half-light radius of $r_{1/2} = 10^{+4}_{-3}$ pc. These properties are consistent with the population of ultra-faint star clusters uncovered by recent surveys. Interestingly, DELVE 6 is located at an angular separation of $\sim 10^{\circ}$ from the center of the Small Magellanic Cloud (SMC), corresponding to a 3D physical separation of ~ 20 kpc given the system's observed distance ($D_{\odot} = 80$ kpc). This also places the system ~ 35 kpc from the center of the Large Magellanic Cloud (LMC), lying within recent constraints on the size of the LMC's dark matter halo. We tentatively measure the proper motion of DELVE 6 using data from Gaia, which we find supports a potential association between the system and the LMC/SMC. Although future kinematic measurements will be necessary to determine its origins, we highlight that DELVE 6 may represent only the second or third ancient ($\tau > 9$ Gyr) star cluster associated with the SMC, or one of fewer than two dozen ancient clusters associated with the LMC. Nonetheless, we cannot currently rule out the possibility that the system is a distant Milky Way halo star cluster.

Unified Astronomy Thesaurus concepts: Star clusters (1567); Magellanic Clouds (990); Sky surveys (1464)

1. Introduction

Recent large-scale digital sky surveys have revolutionized our understanding of the Magellanic Clouds (MCs) and their environments. In particular, sensitive surveys with the VISual

Original content from this work may be used under the terms of the Creative Commons Attribution 4.0 licence. Any further distribution of this work must maintain attribution to the author(s) and the title of the work, journal citation and DOI.

and Infrared Telescope for Astronomy, (e.g., VMC; Cioni et al. 2011), the VLT Survey Telescope (e.g., STEP and YMCA; Ripepi et al. 2014; Gatto et al. 2021), and the Dark Energy Camera (DECam) on the 4 m Blanco Telescope (e.g., DES, SMASH, and MagLiteS; DES Collaboration 2005; Bechtol 2017; Nidever et al. 2017) have provided an unprecedentedly deep view of the diverse stellar populations of the MCs, enabling detailed characterization of their star formation histories (e.g., Rubele et al. 2015, 2018; Mazzi et al. 2021;

Massana et al. 2022), 3D geometries (e.g., Ripepi et al. 2017, 2022; Choi et al. 2018a), and substructures (e.g., Pieres et al. 2017; Choi et al. 2018b; Mackey et al. 2018; Massana et al. 2020; El Youssoufi et al. 2021; Cullinane et al. 2022; Gatto et al. 2022a). Furthermore, these surveys have significantly expanded the census of star clusters and satellite galaxies in the main bodies and outskirts of the Clouds (e.g., Bechtol et al. 2015; Koposov et al. 2015, 2018; Drlica-Wagner et al. 2016; Martin et al. 2016; Torrealba et al. 2018; Cerny et al. 2021a; Gatto et al. 2021), allowing for constraints on the MCs' masses, dark matter halos, orbits, and interaction histories (e.g., Jethwa et al. 2016; Bitsakis et al. 2018; Kallivayalil et al. 2018; Erkal & Belokurov 2020; Patel et al. 2020; Dias et al. 2021), especially when paired with the precise phase-space information provided by the Gaia satellite (Gaia Collaboration et al. 2016; Battaglia et al. 2022; Pace et al. 2022). Lastly, these efforts to survey and characterize the satellite populations of the MCs have enabled novel observational tests of hierarchical galaxy formation within the ACDM paradigm at a lower host mass scale than offered by the Milky Way (MW; e.g., Sales et al. 2016; Dooley et al. 2017; Jahn et al. 2019).

In this Letter, we present the newest discovery in this ongoing census of Magellanic satellites: DELVE 6, an ancient, ultra-faint star cluster in the distant outskirts of the MCs. This low-mass system was identified through matched-filter searches over imaging from DECam (Flaugher et al. 2015) processed as part of the second data release of the DECam Local Volume Exploration survey (DELVE DR2; Drlica-Wagner et al. 2022). We find that it has an old and metal-poor stellar population, joining the less than two dozen ancient globular clusters known in the Magellanic environment, and that it falls at an unusually large separation from its likely hosts. Thus, DELVE 6 potentially represents an exciting and novel window into the stellar populations inhabiting the periphery of the LMC/SMC system. Here we present an initial characterization of this system's basic properties and briefly highlight possibilities for its origins that can be tested with deeper imaging and spectroscopic follow-up.

2. Discovery and Characterization

2.1. Identification in DELVE DR2 and the Legacy Surveys DR10

In Cerny et al. (2023), we presented the results of an extensive search for ultra-faint stellar systems in the MW halo using DECam data processed as part of DELVE DR2 (Drlica-Wagner et al. 2022). Briefly, this search involved applying the open-source simple search code, ²⁸ which implements an isochrone matched filter in color–magnitude space to identify overdensities of resolved stars in the MW halo consistent with an old, metal-poor stellar population. Over the entire DELVE DR2 footprint (\sim 21,000 deg²), this search resulted in $\mathcal{O}(10^4)$ overdensities, six of which we confirmed as bona fide ultrafaint stellar systems in Cerny et al. (2023) on the basis of deeper follow-up imaging.

During the late stages of preparation of the aforementioned work, new multiband coadded images built from the DECam data became available through an early version of the Legacy Surveys Data Release 10.²⁹ Motivated by the new availability

of these images, we performed a visual inspection of a subset of the initial high-significance ($>5.5\sigma$) satellite candidates that resided in regions where comparable color images were not previously available. The primary goal of this effort was to identify systems that were clearly identifiable as overdensities of blue stars in these images but may have initially been missed due to the marginal signals seen in their smoothed spatial distribution and observed color-magnitude diagrams (CMDs) generated as part of simple's diagnostic plots. One such candidate, DELVE J0212-6603 (DELVE 6), was identified at high significance $(6\sigma-7\sigma)$; comparable to the candidates presented in Cerny et al. 2023) in our multipronged search but was initially passed over during prior inspection due to its sparse CMD. However, as seen in Figure 1, this system is visible as a tight clustering of faint blue sources in the color images provided by the Legacy Surveys DR10 and was easily identified during our visual inspection.

After confirming that the system has not been reported in literature catalogs of star clusters and dwarf galaxies in the environment of the MCs (e.g., Bica et al. 2008, 2020; Gatto et al. 2020), we proceeded to characterize the newly discovered system's structure and stellar population, as described in the following subsection. In the absence of timely deeper followup imaging, we continued to use the photometric catalogs provided by DELVE DR2 for our analysis. The DELVE DR2 data coincident with DELVE 6 are relatively deep, reaching (extinction-corrected) S/N = 10 mag limits of $g_0 \sim 24.0$ and $r_0 \sim 23.8$ mag. These limits are roughly 0.5 and 0.8 mag deeper than the median DELVE DR2 depth in the g and r bands, respectively (see Drlica-Wagner et al. 2022 for specific information about this public data set). This depth was therefore found to be sufficient to characterize the newly discovered system despite its low luminosity.

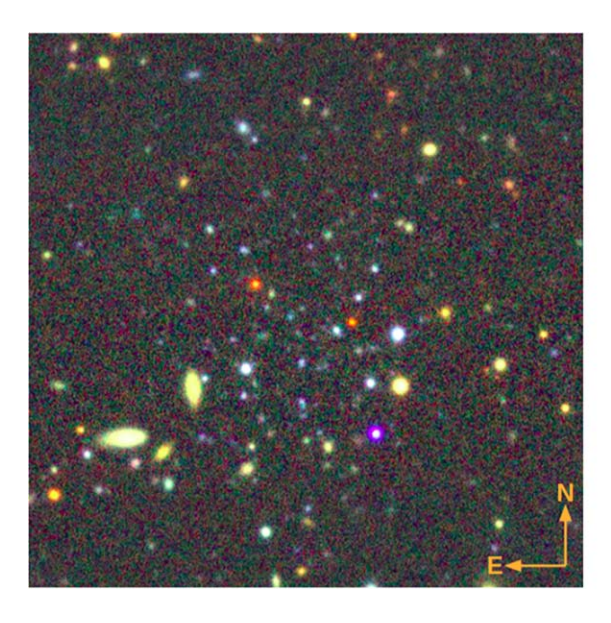
Throughout the analyses described below, we separated stars from galaxies based on the selection $0 \leq \text{EXTENDED}_\text{CLASS_G} \leq 2$, matching our DECam analyses described in Cerny et al. (2023). This broadly allowed for a higher degree of stellar completeness at the cost of increased galaxy contamination at fainter magnitudes (Drlica-Wagner et al. 2022).

2.2. Structural and Stellar Population Fit

We fit DELVE 6's morphological and stellar population properties using the Ultra-faint Galaxy LIkelihood (ugali) software toolkit, which implements an unbinned Poisson maximum-likelihood approach based on the statistical formalism presented in Appendix C of Drlica-Wagner et al. (2020). We modeled DELVE 6's structure with an elliptical Plummer (1911) radial stellar density profile, and we fit a PARSEC isochrone (Bressan et al. 2012) to its observed g- and r-band CMD. The eight free parameters for these models were the centroid coordinates (α_{2000} and δ_{2000}), extension (a_h), ellipticity (ϵ) , and position angle (P.A.) of the Plummer profile and the age (τ) , metallicity ([Fe/H]), and distance modulus $((m-M)_0)$ of the isochrone model. All eight of these parameters were constrained simultaneously by sampling their posterior probability distribution functions using the affine-invariant Markov Chain Monte Carlo (MCMC) ensemble sampler (Goodman & Weare 2010) implemented in the Python package emcee (Foreman-Mackey et al. 2013). This sampling was performed with 80 walkers each taking 35,000 steps, with the first 12,500 steps discarded as burn-in; these parameters were

²⁸ https://github.com/DarkEnergySurvey/simple

https://www.legacysurvey.org/dr10/description/



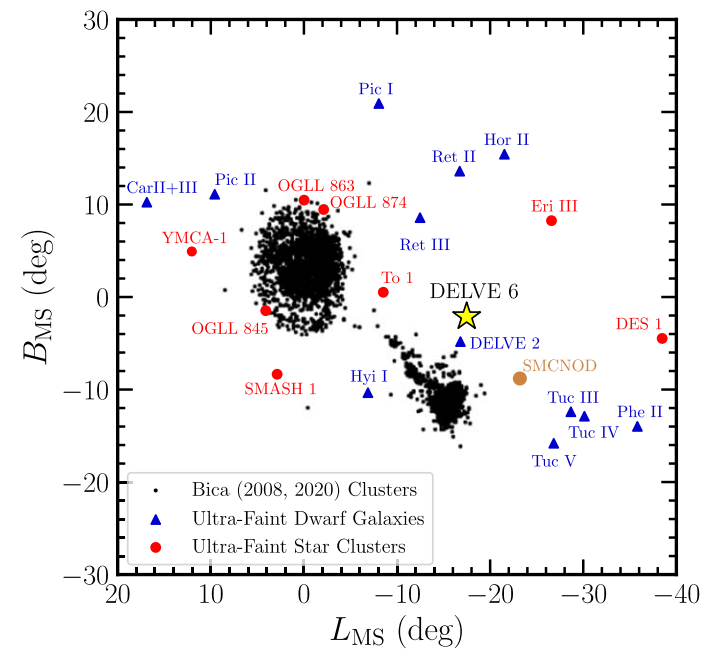


Figure 1. (Left) $2' \times 2'$ false-color image cutout centered on DELVE 6 based on griz DECam imaging, taken from the Legacy Survey Sky Viewer. A clustering of faint blue sources is visible amidst a number of foreground stars and background galaxies. We have increased the brightness of this cutout image to enhance the visibility of faint cluster member stars. (Right) Map of star clusters and dwarf galaxies in the Magellanic environment, plotted in the Magellanic Stream coordinate system from Nidever et al. (2008). Each black point corresponds to a star cluster included in the main cluster catalogs from Bica et al. (2008, 2020). Recently discovered ultra-faint star clusters in this region are shown as red dots, whereas candidate and confirmed ultra-faint dwarf galaxies potentially associated with the MCs are shown as blue triangles. We caution that some of these objects have uncertain classifications and/or tentative associations with the MCs. In addition, we plot the centroid position of the SMC northern overdensity (SMCNOD; Pieres et al. 2017) in orange. Lastly, DELVE 6 is shown as a yellow star positioned near $B_{MS} \sim 0$; this latitude falls along the projected track of the Magellanic Stream.

set to ensure dense sampling of the age-metallicity bimodality described in the next subsection.

We report the best-fit values of each parameter and their associated uncertainties in Table 1. These results were derived from a fit assuming a nominal magnitude limit of g_0 , $r_0 =$ 23.8 mag, and with the size of the concentric annulus used by ugali to construct the foreground/background model used for its joint fit of stellar color, magnitude, and spatial distributions set to 0.5 < r < 1.5. To assess whether these fit hyperparameters might affect our results given the complex, spatially variable foreground/background stellar density associated with the MCs, we explored the sensitivity of our derived estimates of DELVE 6's properties to variations in the assumed magnitude limit and outer radius of the background annulus. Specifically, we reran the full ugali MCMC procedure for magnitude limits in the interval [23.6, 24.0 mag] and background annulus radii in the interval [1°0, 2°0]. In these tests, we found that all fits that converged resulted in parameter estimates consistent within the uncertainties with those reported in Table 1; this was true for all parameters except the P.A., which is mostly unconstrained due to the negligible ellipticity of DELVE 6. However, we did need to apply a weak prior on the extension (sizes $0.001 < a_h < 0.1$) in order to avoid convergence to nonphysical results. Our fiducial results presented in Table 1 were derived with this prior applied.

2.3. Properties of DELVE 6

As depicted in Figures 2 and 3, we find that DELVE 6 is a compact $(r_{1/2}=10^{+4}_{-3} \text{ pc})$, ultra-faint $(M_V=-1.5^{+0.4}_{-0.6} \text{ mag})$ stellar system with a round morphology $(\epsilon < 0.56$ at 95% confidence). These properties place DELVE 6 in a region of the M_V - $r_{1/2}$ plane that is dominated by the population of

ultra-faint MW halo star clusters discovered by recent surveys, which are generally fainter and more compact than their ultra-faint dwarf galaxy counterparts (see Figure 4). We do observe that DELVE 6 is among the more extended (candidate) ultra-faint star clusters discovered to date, though. We tentatively classify DELVE 6 as an ultra-faint star cluster on the basis of its small physical size, although a future spectroscopic measurement of its velocity and/or metallicity dispersion will provide a more definitive classification for the system.

In addition, we find that DELVE 6 is most consistent with an ancient stellar population, as is evident from the clear mainsequence turnoff, extended subgiant branch, and (sparse) red giant branch (RGB) seen in its observed CMD (Figures 2 and 3). The best-fit isochrone favored by our ugali fit was consistent with the maximum age and minimum metallicity of our isochrone grid $(\tau = 13.5 \, \text{Gyr} \text{ and } [\text{Fe/H}] = -2.19 \, \text{dex}, \text{ respectively}), \text{ although}$ the marginalized posterior distribution for these two parameters was found to be bimodal, with a secondary peak at $\tau \sim 10\,\mathrm{Gyr}$ and $[Fe/H] \sim -1.2$ dex (see left panel of Figure 3). These modes appear to depend on whether the single blue horizontal branch (BHB) star candidate shown in the right panel of Figure 3 is a true member or, alternately, whether the star positioned near the red horizontal branch (RHB) of the second model is a true member. In our nominal best-fit parameter constraints, the BHB star is included as a high-confidence member, driving the fit toward the lower-metallicity mode (blue isochrone in Figure 3). Removing the BHB star from our photometric catalog and rerunning the fit resulted in the secondary mode becoming the favored best-fit solution (red isochrone in the same figure). If we instead removed the candidate RHB star, the results are qualitatively similar to those shown in Figure 3.

Using the BHB-blue straggler separation technique introduced in Li et al. (2019), we found that the BHB star's

Table 1 Properties of DELVE 6

Parameter	Value	Units	
IAU name	DELVE J0212-6603		
Constellation	Hydrus	•••	
α_{2000}	$33.070^{+0.003}_{-0.004}$	deg	
δ_{2000}	$-66.056^{+0.002}_{-0.002}$	deg	
r_h	$0.43^{+0.18}_{-0.12}$	arcmin	
$r_{1/2}$	10^{+4}_{-3}	pc	
ϵ	< 0.56		
P.A.	14^{+40}_{-63}	deg	
M_V^{a}	$-1.5^{+0.4}_{-0.6}$	mag	
au	>9.8	Gyr	
[Fe/H]	<-1.17	dex	
$(m-M)_0$	$19.51^{+0.04}_{-0.12}$ (stat.) $\pm 0.1^{\rm b}$ (sys.)	mag	
D_{\odot}	80^{+2}_{-4} (stat.) $^{+4}_{-4}$ (sys.)	kpc	
D_{GC}	78^{+2}_{-4} (stat.) $^{+4}_{-4}$ (sys.)	kpc	
$D_{ m LMC}$	35^{+2}_{-3} (stat.) $^{+3}_{-3}$ (sys.)	kpc	
$D_{ m SMC}$	20^{+2}_{-3} (stat.) $^{+3}_{-3}$ (sys.)	kpc	
$E(B-V)^{c}$	0.036	mag	
$\mu_{\alpha}\cos\delta$	$0.93^{+0.39}_{-0.39}$	mas yr ⁻¹	
μ_{δ}	$-1.28^{+0.38}_{-0.38}$	mas yr ⁻¹	

Notes. Uncertainties for each parameter were derived from the highest-density interval containing 68% of the marginalized posterior distribution. For the ellipticity, metallicity, and age, the posterior distribution peaked at the boundary of the allowed parameter space. Therefore, we quote the upper, upper, and lower bound for these three parameters, respectively, at 95% confidence.

 $(g-r)_0$ and $(i-z)_0$ color is consistent with a classification as a bona fide BHB star. Furthermore, the star's Gaia DR3 proper motion (Gaia Collaboration et al. 2023) is sufficiently small that we cannot clearly identify it as a foreground star, and its parallax is consistent with zero within errors; we therefore cannot rule out its membership in the distant DELVE 6 system. By contrast, the RHB candidate's proper motion of $(\mu_{\alpha} \cos \delta, \, \mu_{\delta}) = (-3.0 \pm 0.4, \, -12.2 \pm 0.3)$ implies a tangential velocity that is inconsistent with that of a typical star in a bound orbit at DELVE 6's distance; this suggests that the star is not a member of DELVE 6. We have opted to present our ugali fit results from a fit with both stars included in our catalog. This decision fully specifies the age/metallicity solution that we report for DELVE 6 due to the strong impact of the BHB candidate, but the upper/lower limits presented in the Table 1 encompass both plausible solutions for these two parameters. Despite the uncertainty in the age and metallicity, we found that the structural properties presented in Table 1 are consistent within uncertainties with the results derived from fits with either one of the two stars in question removed.

Although we cannot conclusively determine which age/metallicity is most appropriate for DELVE 6 until deeper imaging and/or a spectroscopic metallicity measurement becomes available, both of these isochrone fits strongly suggest that the system is ancient ($\tau > 9.8$ Gyr). DELVE 6's old age, as

well as its position in the outskirts of the LMC and SMC, raises interesting questions about its formation and evolution. We study the systemic proper motion of DELVE 6 below and then explore several possibilities for its origin in Section 3.

2.4. Systemic Proper Motion of DELVE 6

In addition to the aforementioned BHB and RHB candidates. we identified one additional nearby member candidate with a Gaia proper-motion measurement. This star (Gaia DR3 source_id: 4698076296289956352) is the brightest RGB star consistent with our best-fit isochrone in Figure 2 and was identified as a high-probability member in our ugali fit ($p_{\rm ugali}=0.99$; see Appendix A, Table 2). Notably, this RGB star's proper motion is consistent with the BHB star at the 1.3σ level.³⁰ The adequate agreement in proper motion supports the interpretation that the BHB and RGB stars may both be members of DELVE 6, as the joint probability of having these two stars lying by chance on a single isochrone while also sharing a statistically consistent nonzero proper motion is small. It is thus reasonable to derive the proper motion of DELVE 6 from these two stars, which we find to be yr^{-1} $(\mu_{\alpha}\cos\delta, \mu_{\delta}) = (0.93 \pm 0.39, -1.28 \pm 0.38)$ mas through a simple two-parameter fit.

Although this measurement is tentative and should be interpreted cautiously, DELVE 6's kinematics are singularly important for unraveling its origins. Therefore, we briefly explored what this measurement might tell us about the connection of DELVE 6 to possible host systems. To do so, we calculated its azimuthal and polar velocity components in galactocentric spherical coordinates (hereafter v_{ϕ} and v_{θ}) by sampling from the posterior distributions for the available 5D phase-space measurements and sampling the unknown radial velocity from a uniform distribution on the interval [-500, 500 km s⁻¹]. We then compared the values of these velocity components to those expected from stars belonging to the distant MW halo and the MCs.

Using galpy (Bovy 2015) to carry out the velocity transformation, we find $v_{\phi} = -50 \pm 150$, $v_{\theta} = -430 \pm$ 150 km s⁻¹, where the best-fit values and the upper/lower uncertainties correspond to the median and 16th/84th percentiles across 100,000 random 6D samples. This value of v_{ϕ} is uninformative, as it is consistent with the expected velocity distributions of all three hosts. However, we do observe that DELVE 6's estimated polar velocity v_{θ} is approximately consistent with that of the LMC $(v_{\theta} \sim -305 \text{ km s}^{-1})$ and SMC $(v_{\theta} \sim$ -260 km s^{-1}). The polar velocity distribution of MW halo tracers at 80 kpc is expected to be a Gaussian centered near $v_{\theta} = 0 \text{ km}^{-1}$ with dispersion $\sigma_{\nu_{\theta}} \lesssim 100 \text{ km s}^{-1}$ (see Figure 4 of Bird et al. 2019); thus, DELVE 6 appears to be kinematically distinct from typical stars in the outer halo in this velocity component. We therefore conclude that DELVE 6's proper motion, taken at face value, would argue in favor of a Magellanic association. This conclusion only weakly depends on the unknown line-of-sight velocity but is limited by the large error on DELVE 6's proper motion. Reduced proper-motion errors (e.g., from future Gaia data releases) will provide more definitive kinematic evidence for an association with one host or another.

^a Our estimate of M_V was derived following the procedure from Martin et al. (2008) and does not include the uncertainty in the distance.

^b The statistical uncertainty on DELVE 6's distance is derived directly from our ugali MCMC. We include a systematic uncertainty of ± 0.1 associated with isochrone modeling following Drlica-Wagner et al. (2015). This systematic error is not included in the uncertainty on $r_{1/2}$.

^c This E(B-V) value is the mean reddening of all sources within $r_{1/2}$, as determined via the maps of Schlegel et al. (1998) with the recalibration from Schlafly & Finkbeiner (2011).

 $[\]overline{^{30}}$ Here the confidence level calculated appropriately for the case of 2D Gaussians was converted to the equivalent σ distance for a 1D Gaussian; however, this calculation neglects the covariance between proper-motion components.

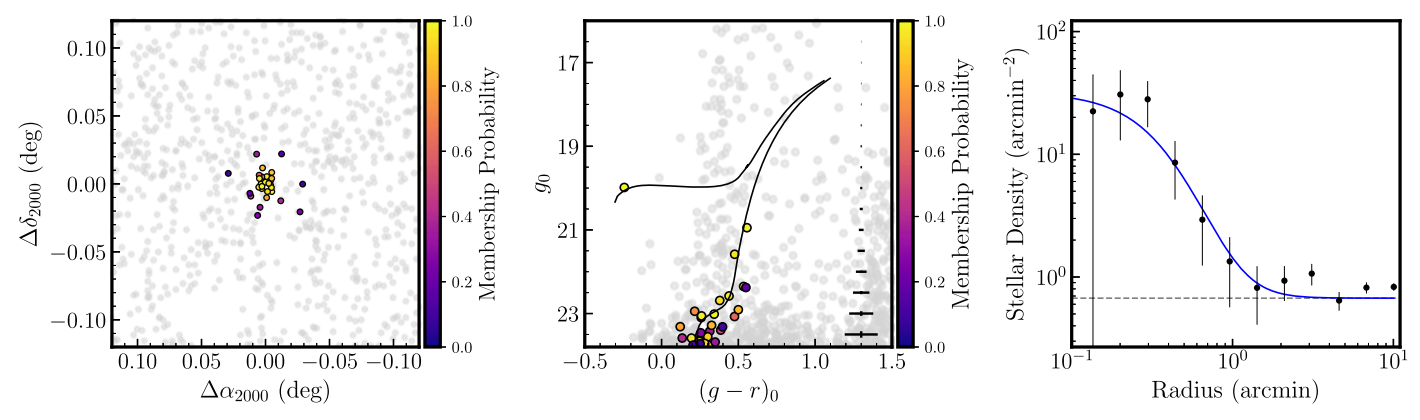


Figure 2. (Left) Spatial distribution of stars in a $0^{\circ}.12 \times 0^{\circ}.12 \times 0^{\circ}.12 \times 7^{\circ}.2$) field centered on DELVE 6. Stars are colored by their probability of being a member of the candidate system, as determined through our ugali fit described in Section 2.2; stars with probabilities p < 0.1 are shown in gray. (Middle) CMD for the stars shown in the left panel. The best-fit isochrone with Z = 0.0001 and $\tau = 13.5$ Gyr is shown in black, although see the discussion in Section 2.2 and Figure 3 for caveats about this model. (Right) Radial stellar density profile for DELVE 6. The best-fit Plummer model is shown as a solid blue curve, assuming the half-light radius reported in Table 1 and an ellipticity $\epsilon = 0$. This ellipticity is approximately matched to the mode of the marginalized posterior distribution for ϵ derived from our MCMC analysis; however, our constraint on the system's ellipticity ($\epsilon < 0.56$ at 95% confidence) is relatively weak due to the small number of observed member stars.

3. Discussion

At its projected sky position (Figure 1) and galactocentric distance ($D_{GC} = 78 \text{ kpc}$), DELVE 6 is located 20 kpc from the center of the SMC and 35 kpc from the center of the LMC.³¹ Despite this relative proximity, DELVE 6 is located beyond the tidal radius (r_t) of the LMC due to the MW $(r_t \sim 22 \text{ kpc})$; van der Marel & Kallivayalil 2014) and the tidal radius of the SMC due to the LMC ($r_t \sim 5 \text{ kpc}$; Massana et al. 2020), suggesting that these two possible hosts have a weak gravitational influence on DELVE 6. It is therefore not immediately evident based on its position alone whether this system is associated with either of the Clouds. On the basis of its separation from the LMC and SMC, as well as the possible ages and metallicities discussed above, we speculate that DELVE 6 is most likely described by one of three scenarios: (1) a distant ultra-faint MW halo star cluster coincidentally located near the MCs, (2) an LMC cluster residing in its host's outer halo in a weakly bound or unbound orbit, or (3) a cluster formed within the SMC that has been stripped from its host and now orbits in the MW+LMC potential.

The first of these scenarios is supported by the similarity between DELVE 6's age and metallicity to the properties of the MW's "classical" globular clusters and the growing population of ultra-faint MW halo star clusters. This scenario also mitigates the need for an explanation of DELVE 6's apparently large separation from the LMC and SMC. Roughly a dozen MW star clusters are known at $D_{\odot} > 70$ kpc, suggesting that an LMC/SMC origin is not necessary to explain DELVE 6's large galactocentric distance. This all being said, our exploration of DELVE 6's tentative proper motion (Section 2.4) suggests that its overall kinematics may be more consistent with the LMC/SMC system and inconsistent with MW halo tracers at its distance.

On that note, the second of our proposed scenarios—namely, that the system was formed in the LMC and remains in a weakly bound or unbound orbit around its host—may also explain the

ancient age of DELVE 6 given the \sim 15 known LMC globular clusters with ages >9 Gyr (e.g., Mackey & Gilmore 2004) but does not directly explain the system's present-day galactocentric distance and 3D separation. Indeed, if confirmed to be an LMC satellite, DELVE 6 would reside at a larger separation from the LMC than all but two star clusters believed to be associated with the MCs.³³ Nevertheless, there is evidence that the LMC dark matter halo extends >50 kpc in radius (e.g., Koposov et al. 2023), making it plausible that DELVE 6 lies in the outskirts of the LMC halo. Furthermore, we note that at least two ultra-faint dwarf galaxies that are likely to be associated with the LMC lie at larger separations from their (original) host compared to DELVE 6: Horologium I and Phoenix II (see Pace et al. 2022). Detailed modeling of the MW and LMC dark matter halo structures (including the LMC's dynamical friction wake) and these satellites' orbits within the associated potential suggests that the former of these two ultra-faint dwarfs is unbound from the LMC, while the latter is likely bound (Garavito-Camargo et al. 2021). By analogy, we conclude that DELVE 6 could plausibly be either weakly bound to the LMC or unbound, given its current position.

The last possibility is that DELVE 6 was initially formed within the SMC but was stripped from its host due to interactions between the LMC and SMC. The strongest (and arguably only) observational evidence for this conclusion is DELVE 6's large present-day galactocentric distance and its on-sky location. These properties place the system in a 3D position where a relatively high density of SMC satellites/debris is expected based on numerical simulations (Jethwa et al. 2016). In further support of this possibility, we highlight that a similar stripping scenario has also been proposed for the recently discovered ultra-faint star cluster YMCA-1 on the basis of its proper motion (Piatti & Lucchini 2022); like DELVE 6, this system lies well beyond the SMC's tidal radius.

Disfavoring this stripping scenario is the fact that DELVE 6's age and metallicity from our nominal best-fit solution are inconsistent with the known SMC globular cluster population, which includes only a single comparably old system with a robustly measured age (NGC 121, at $\tau \sim 11$ Gyr; Glatt et al.

 $[\]overline{^{31}}$ We assume galactocentric distances for the LMC, SMC, and Galactic center from Pietrzyński et al. (2013), Graczyk et al. (2020), and GRAVITY Collaboration et al. (2019), respectively. We neglect the uncertainties on these distances and on each object's centroid coordinates when calculating $D_{\rm LMC}$, $D_{\rm SMC}$, and $D_{\rm GC}$ because they are subdominant relative to the uncertainty on DELVE 6's heliocentric distance.

³² This number includes ultra-faint systems but excludes clusters in the MW's dwarf satellites (e.g., those in the Fornax dSph and Eridanus II).

³³ The two candidate LMC/SMC clusters at larger separations are DES 1 (Luque et al. 2016) and Eridanus III (Bechtol et al. 2015); both are included in Figure 1. Conn et al. (2018) argued in favor of a Magellanic association for both, although their analysis did not rely on any kinematic evidence.

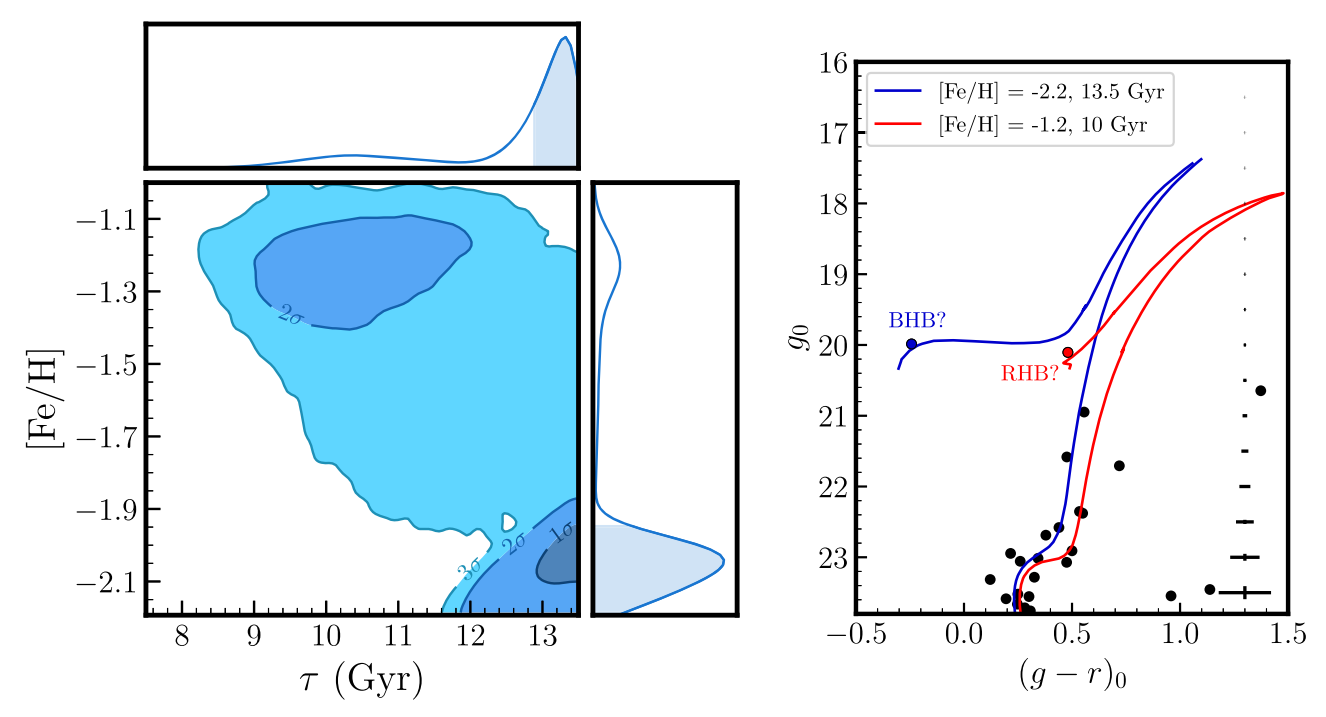


Figure 3. (Left) 2D posterior probability distribution for the metallicity and age of DELVE 6. The blue shaded contours denote the 1σ , 2σ , and 3σ 2D confidence regions in this plane. (Right) CMD for all stars within $2r_{1/2}$ of DELVE 6's centroid. Two isochrone models are shown. The blue model depicts an isochrone with [Fe/H] = -2.19 and $\tau = 13.5$ Gyr, consistent with the posterior mode shown in the bottom right corner of the left panel, whereas the red model depicts a younger, more metal-rich isochrone corresponding to a fit lying within the medium-blue 2σ contour near the top center of the left panel. Here both models are fixed to the distance modulus reported in Table 1, despite small differences in distance between the corresponding samples. We highlight that one BHB candidate lies along the older, more metal-poor (blue) model, and one (likely nonmember) star lies near the RHB of the younger, more metal-rich (red) model.

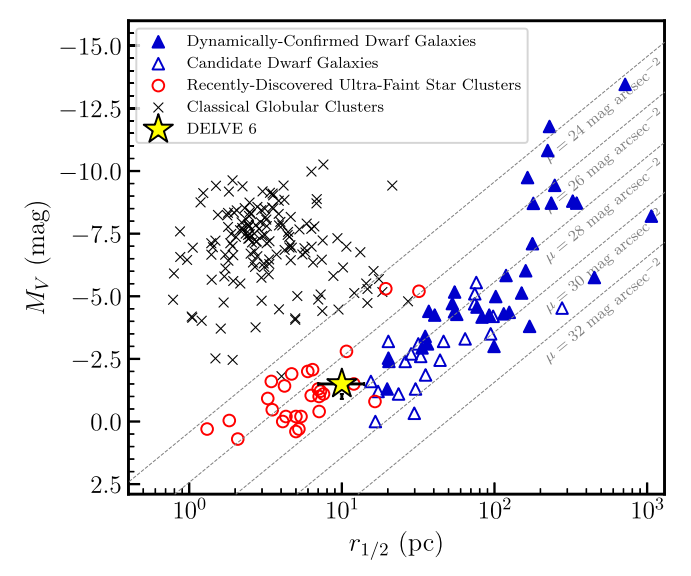


Figure 4. Absolute magnitude (M_V) vs. azimuthally averaged half-light radius $(r_{1/2})$ for a large sample of classical globular clusters, candidate and confirmed MW satellite galaxies, and recently discovered ultra-faint halo star clusters. The location of DELVE 6 in this plane is indicated by a yellow star. A complete reference list for this figure is available in Appendix B.

2008). Indeed, our measurement suggests that DELVE 6 would be the second- or third-oldest star cluster associated with the SMC, depending on the status of the aforementioned YMCA-1 system, which has a somewhat uncertain age ($\tau \sim 9.6$ –11.7 Gyr; Gatto et al. 2022b; Piatti & Lucchini 2022) and only a tentative association with the SMC. Nonetheless, such a stripping scenario has been proposed as one explanation for the apparent dearth of old star clusters associated with the SMC. By tracing the orbits of star clusters throughout a period

of dynamical interaction between the LMC and SMC, Carpintero et al. (2013) found that for large eccentricities (e > 0.5), $\sim 15\%$ of the SMC star clusters are captured by the LMC, and an additional $\sim 20\%$ –50% of the clusters are ejected into the intergalactic medium. We believe that either of these two capture scenarios is more likely than the possibility that DELVE 6 inhabits a weakly bound orbit in the outer halo of the SMC (analogous to the case above for the LMC) given that the system lies at $\sim 4r_{t, \text{SMC}}$ compared to $\sim 1.6r_{t, \text{LMC}}$.

Spectroscopic follow-up will be critical for distinguishing between these scenarios. Specifically, a radial velocity measurement would enable the possibility of rewinding DELVE 6's orbit in the combined MW+LMC+SMC potential, elucidating its origins. If an LMC or SMC origin can be robustly established on the basis of its orbit, DELVE 6 may provide a significant constraint on its host's age—metallicity relation at a very large radius. Deeper imaging reaching the main-sequence turnoff feature of DELVE 6's CMD will be necessary to realize this possibility and robustly confirm this system's ancient age, and a spectroscopic metallicity measurement would aid in breaking the age—metallicity degeneracy inherent to isochrone fitting.

Lastly, we highlight that the discovery of DELVE 6 emphasizes that the observational census of ultra-faint systems in the Magellanic environment is incomplete. In the near term, DELVE's Magellanic Cloud survey component (DELVE-MC; see Drlica-Wagner et al. 2021) will provide deep, homogeneous imaging spanning ~2170 deg² over this region of sky, enabling a comprehensive search for ultra-faint systems in the MCs and their outskirts. Considering the continual discovery of ultra-faint star clusters near the MCs in recent years, we speculate that a more extensive population of old, metal-poor, ultra-faint star clusters may exist around the LMC, SMC, and

perhaps even other low-mass galaxies in the Local Group, waiting to be uncovered by current and future surveys.

Acknowledgments

The code and data products associated with this work are archived on Zenodo: doi:10.5281/zenodo.8213406.

This project is partially supported by the NASA Fermi Guest Investigator Program Cycle 9 No. 91201. This work is partially supported by Fermilab LDRD project L2019-011. W.C. gratefully acknowledges support from a Gruber Science Fellowship at Yale University. C.E.M.V. is supported by the international Gemini Observatory, a program of NSF's NOIRLab, which is managed by the Association of Universities for Research in Astronomy (AURA) under a cooperative agreement with the National Science Foundation, on behalf of the Gemini partnership of Argentina, Brazil, Canada, Chile, the Republic of Korea, and the United States of America. J.A.C.-B. acknowledges support from FONDECYT Regular No. 1220083.

This project used data obtained with the Dark Energy Camera, which was constructed by the Dark Energy Survey (DES) collaboration. Funding for the DES Projects has been provided by the DOE and NSF (USA), MISE (Spain), STFC (UK), HEFCE (UK), NCSA (UIUC), KICP (U. Chicago), CCAPP (Ohio State), MIFPA (Texas A&M University), CNPQ, FAPERJ, FINEP (Brazil), MINECO (Spain), DFG (Germany), and the collaborating institutions in the Dark Energy Survey, which are Argonne Lab, UC Santa Cruz, University of Cambridge, CIEMAT-Madrid, University of Chicago, University College London, DES-Brazil Consortium, University of Edinburgh, ETH Zürich, Fermilab, University of Illinois, ICE (IEEC-CSIC), IFAE Barcelona, Lawrence Berkeley Lab, LMU München, and the associated Excellence Cluster Universe, University of Michigan, NSF's National Optical-Infrared Astronomy Research Laboratory, University of Nottingham, Ohio State University, OzDES Membership Consortium University of Pennsylvania, University of Portsmouth, SLAC National Lab, Stanford University, University of Sussex, and Texas A&M University.

Based on observations at Cerro Tololo Inter-American Observatory, NSF's National Optical-Infrared Astronomy Research Laboratory (2019A-0305; PI: Drlica-Wagner), which is operated by the Association of Universities for Research in Astronomy (AURA) under a cooperative agreement with the National Science Foundation.

The Legacy Surveys consist of three individual and complementary projects: the Dark Energy Camera Legacy Survey (DECaLS; Proposal ID 2014B-0404; PIs: David Schlegel and Arjun Dey), the Beijing-Arizona Sky Survey (BASS; NOAO Prop. ID 2015A-0801; PIs: Zhou Xu and Xiaohui Fan), and the Mayall z-band Legacy Survey (MzLS; Prop. ID 2016A-0453; PI: Arjun Dey). DECaLS, BASS, and MzLS together include data obtained, respectively, at the Blanco telescope, Cerro Tololo Inter-American Observatory, NSFs NOIRLab; the Bok telescope, Steward Observatory, University of Arizona; and the Mayall telescope, Kitt Peak National Observatory, NOIRLab. Pipeline processing and analyses of the data were supported by NOIRLab and the Lawrence Berkeley National Laboratory (LBNL). The Legacy Surveys project is honored to be permitted to conduct astronomical research on Iolkam Du'ag (Kitt Peak), a mountain with particular significance to the Tohono O'odham Nation.

NOIRLab is operated by the Association of Universities for Research in Astronomy (AURA) under a cooperative agreement with the National Science Foundation. LBNL is managed by the Regents of the University of California under contract to the US Department of Energy.

BASS is a key project of the Telescope Access Program (TAP), which has been funded by the National Astronomical Observatories of China, the Chinese Academy of Sciences (Strategic Priority Research Program "The Emergence of Cosmological Structures" grant No. XDB09000000), and the Special Fund for Astronomy from the Ministry of Finance. BASS is also supported by the External Cooperation Program of the Chinese Academy of Sciences (grant No. 114A11KYSB20160057) and the Chinese National Natural Science Foundation (grant Nos. 12120101003 and 11433005).

The Legacy Survey team makes use of data products from the Near-Earth Object Wide-field Infrared Survey Explorer (NEOWISE), which is a project of the Jet Propulsion Laboratory/California Institute of Technology. NEOWISE is funded by the National Aeronautics and Space Administration.

The Legacy Surveys imaging of the DESI footprint is supported by the Director, Office of Science, Office of High Energy Physics of the US Department of Energy under contract No. DE-AC02-05CH1123; the National Energy Research Scientific Computing Center, a DOE Office of Science User Facility under the same contract; and the US National Science Foundation, Division of Astronomical Sciences under contract No. AST-0950945 to NOAO.

This work has made use of data from the European Space Agency (ESA) mission Gaia (https://www.cosmos.esa.int/gaia), processed by the Gaia Data Processing and Analysis Consortium (DPAC; https://www.cosmos.esa.int/web/gaia/dpac/consortium). Funding for the DPAC has been provided by national institutions, in particular the institutions participating in the Gaia Multilateral Agreement.

This work made use of Astropy,³⁴ a community-developed core Python package and an ecosystem of tools and resources for astronomy.

This manuscript has been authored by the Fermi Research Alliance, LLC, under contract No. DE-AC02-07CH11359 with the US Department of Energy, Office of Science, Office of High Energy Physics. The United States Government retains and the publisher, by accepting the article for publication, acknowledges that the United States Government retains a nonexclusive, paidup, irrevocable worldwide license to publish or reproduce the published form of this manuscript, or allow others to do so, for United States Government purposes.

Facilities: Blanco, Gaia.

Software: numpy (van der Walt et al. 2011; Harris et al. 2020), scipy (Virtanen et al. 2020), emcee (Foreman-Mackey et al. 2013), HEALPix (Górski et al. 2005), 35 healpy (Zonca et al. 2019), ugali (Bechtol et al. 2015), 6 ChainConsumer (Hinton 2019), simple (Bechtol et al. 2015; Drlica-Wagner et al. 2015), astropy (Astropy Collaboration et al. 2013, 2018, 2022).

Appendix A Candidate DELVE 6 Members Identified in Gaia DR3

In Table 2, we summarize the properties of the three potential DELVE 6 member stars that we identified in Gaia

³⁴ http://www.astropy.org

³⁵ http://healpix.sourceforge.net

³⁶ https://github.com/DarkEnergySurvey/ugali

Table 2 Properties of Candidate Proper-motion Members of DELVE 6

Gaia Source ID	R.A. (deg)	Decl. (deg)	ϖ (mas)	$\mu_{\alpha}\cos\delta$ (mas yr ⁻¹)	μ_{δ} (mas yr ⁻¹)	$p_{ m ugali}$	Comment
4698076296289954048	33.0582	-66.0618	0.0 ± 0.4	$0.6{\pm}0.5$	-1.1 ± 0.4	1.00	BHB candidate
4698076296289956352	33.0771	-66.0579	0.2 ± 0.6	2.0 ± 0.8	-2.2 ± 0.9	0.99	RGB star
4698076296289957248	33.0549	-66.0558	0.0 ± 0.3	-3.0 ± 0.4	-12.2 ± 0.3	0.00	RHB? nonmember

Note. The astrometric properties included above are all taken directly from Gaia DR3. Here p_{ugali} is the membership probability of each star (rounded to the nearest hundredth) as determined from our fiducial results, which favored the isochrone model with $\tau = 13.5$ Gyr and [Fe/H] = -2.19 dex.

DR3. We refer the reader to Section 2.2 for a more detailed discussion of these sources.

Appendix B References for Literature Data Presented in Figure 4

In Figure 4, we compare DELVE 6's absolute V-band magnitude (M_V) and azimuthally averaged half-light radius $(r_{1/2})$ to the known population of MW satellite galaxies, globular clusters, and recently discovered ultra-faint star clusters. For the MW satellite galaxies, we adopted or derived measurements of M_V and $r_{1/2}$ from McConnachie (2012), Kim & Jerjen (2015a), Drlica-Wagner et al. (2015), Koposov et al. (2015, 2018), Martin et al. (2015), Torrealba et al. (2016a, 2016b, 2018), Crnojević et al. (2016), Drlica-Wagner et al. (2016), Carlin et al. (2017), Homma et al. (2016, 2018, 2019), Muñoz et al. (2018), Mutlu-Pakdil et al. (2018), Wang et al. (2019), Mau et al. (2020), Moskowitz & Walker (2020), Simon et al. (2020), Cerny et al. (2021b, 2023), Ji et al. (2021), Cantu et al. (2021), Richstein et al. (2022), and Cerny et al. (2023). For the ultra-faint star clusters, we adopted or derived measurements from Fadely et al. (2011), Muñoz et al. (2012, 2018), Balbinot et al. (2013), Kim & Jerjen (2015b), Kim et al. (2015, 2016), Martin et al. (2016), Weisz et al. (2016), Conn et al. (2018), Longeard et al. (2018, 2019), Luque et al. (2018), Mutlu-Pakdil et al. (2018), Homma et al. (2019), Mau et al. (2019, 2020), Torrealba et al. (2019), Cerny et al. (2021a, 2023), and Gatto et al. (2022b). In cases where the above studies of ultra-faint systems quote only an elliptical half-light radius, we have converted these measurements to azimuthally averaged half-light radii using these works' reported ellipticities (where possible). Lastly, measurements for the classical globular clusters are taken from Harris (2010). Two ultra-faint star clusters discovered in the Sloan Digital Sky Survey (Koposov 1 and Koposov 2; Koposov et al. 2007) have been removed from this catalog to avoid duplication.

ORCID iDs

W. Cerny https://orcid.org/0000-0003-1697-7062 A. Drlica-Wagner https://orcid.org/0000-0001-8251-933X T. S. Li https://orcid.org/0000-0002-9110-6163 A. B. Pace https://orcid.org/0000-0002-6021-8760 K. A. G. Olsen https://orcid.org/0000-0002-7134-8296 N. E. D. Noël https://orcid.org/0000-0002-8282-469X R. P. van der Marel https://orcid.org/0000-0001-7827-7825 J. L. Carlin https://orcid.org/0000-0002-3936-9628 Y. Choi https://orcid.org/0000-0003-1680-1884 D. Erkal https://orcid.org/0000-0002-8448-5505 M. Geha https://orcid.org/0000-0002-7007-9725 D. J. James https://orcid.org/0000-0001-5160-4486 C. E. Martínez-Vázquez https://orcid.org/0000-0002-

9144-7726 P. Massana https://orcid.org/0000-0002-8093-7471

510, 445 DES Collaboration 2005, arXiv:astro-ph/0510346 Dias, B., Angelo, M. S., Oliveira, R. A. P., et al. 2021, A&A, 647, L9

Dooley, G. A., Peter, A. H. G., Carlin, J. L., et al. 2017, MNRAS, 472, 1060 Drlica-Wagner, A., Bechtol, K., Allam, S., et al. 2016, ApJL, 833, L5 Drlica-Wagner, A., Bechtol, K., Rykoff, E. S., et al. 2015, ApJ, 813, 109 Drlica-Wagner, A., Carlin, J. L., Nidever, D. L., et al. 2021, ApJS, 256, 2 Drlica-Wagner, A., Ferguson, P. S., Adamów, M., et al. 2022, ApJS, 261, 38 El Youssoufi, D., Cioni, M.-R. L., Bell, C. P. M., et al. 2021, MNRAS,

505, 2020 Erkal, D., & Belokurov, V. A. 2020, MNRAS, 495, 2554 Fadely, R., Willman, B., Geha, M., et al. 2011, AJ, 142, 88 Flaugher, B., Diehl, H. T., Honscheid, K., et al. 2015, AJ, 150, 150 Foreman-Mackey, D., Hogg, D. W., Lang, D., & Goodman, J. 2013, PASP,

G. E. Medina https://orcid.org/0000-0003-0105-9576 A. E. Miller https://orcid.org/0000-0002-7483-7327 B. Mutlu-Pakdil https://orcid.org/0000-0001-9649-4815 D. L. Nidever https://orcid.org/0000-0002-1793-3689

J. D. Sakowska https://orcid.org/0000-0002-1594-1466

G. S. Stringfellow https://orcid.org/0000-0003-1479-3059

J. A. Carballo-Bello https://orcid.org/0000-0002-3690-105X P. S. Ferguson https://orcid.org/0000-0001-6957-1627

N. Kuropatkin https://orcid.org/0000-0003-2511-0946

S. Mau https://orcid.org/0000-0003-3519-4004 E. J. Tollerud https://orcid.org/0000-0002-9599-310X

A. K. Vivas https://orcid.org/0000-0003-4341-6172

References

Astropy Collaboration, Price-Whelan, A. M., Lim, P. L., et al. 2022, ApJ,

Astropy Collaboration, Price-Whelan, A. M., Sipőcz, B. M., et al. 2018, AJ, 156, 123

Astropy Collaboration, Robitaille, T. P., Tollerud, E. J., et al. 2013, A&A, 558. A33

Balbinot, E., Santiago, B. X., da Costa, L., et al. 2013, ApJ, 767, 101 Battaglia, G., Taibi, S., Thomas, G. F., & Fritz, T. K. 2022, A&A, 657, A54 Bechtol, K. 2017, AAS Meeting Abstracts, 229, 416.06

Bechtol, K., Drlica-Wagner, A., Balbinot, E., et al. 2015, ApJ, 807, 50 Bica, E., Bonatto, C., Dutra, C. M., & Santos, J. F. C. 2008, MNRAS, 389, 678

Bica, E., Westera, P., Kerber, L. d. O., et al. 2020, AJ, 159, 82 Bird, S. A., Xue, X.-X., Liu, C., et al. 2019, AJ, 157, 104

Bitsakis, T., González-Lópezlira, R. A., Bonfini, P., et al. 2018, ApJ, 853, 104 Bovy, J. 2015, ApJS, 216, 29

Bressan, A., Marigo, P., Girardi, L., et al. 2012, MNRAS, 427, 127 Cantu, S. A., Pace, A. B., Marshall, J., et al. 2021, ApJ, 916, 81

Carlin, J. L., Sand, D. J., Muñoz, R. R., et al. 2017, AJ, 154, 267 Carpintero, D. D., Gomez, F. A., & Piatti, A. E. 2013, MNRAS, 435, L63

Cerny, W., Martínez-Vázquez, C. E., Drlica-Wagner, A., et al. 2023, ApJ, Cerny, W., Pace, A. B., Drlica-Wagner, A., et al. 2021a, ApJ, 910, 18

Cerny, W., Pace, A. B., Drlica-Wagner, A., et al. 2021b, ApJL, 920, L44

Cerny, W., Simon, J. D., Li, T. S., et al. 2023, ApJ, 942, 111 Choi, Y., Nidever, D. L., Olsen, K., et al. 2018a, ApJ, 866, 90

Choi, Y., Nidever, D. L., Olsen, K., et al. 2018b, ApJ, 869, 125

Cioni, M. R. L., Clementini, G., Girardi, L., et al. 2011, A&A, 527, A116 Conn, B. C., Jerjen, H., Kim, D., & Schirmer, M. 2018, ApJ, 852, 68

Crnojević, D., Sand, D. J., Zaritsky, D., et al. 2016, ApJL, 824, L14 Cullinane, L. R., Mackey, A. D., Da Costa, G. S., et al. 2022, MNRAS,

Drlica-Wagner, A., Bechtol, K., Mau, S., et al. 2020, ApJ, 893, 47

```
Gaia Collaboration, Prusti, T., de Bruijne, J. H. J, et al. 2016, A&A, 595, A1
Gaia Collaboration, Vallenari, A., Brown, A. G. A., et al. 2023, A&A, 674, A1
Garavito-Camargo, N., Besla, G., Laporte, C. F. P., et al. 2021, ApJ, 919, 109
Gatto, M., Ripepi, V., Bellazzini, M., et al. 2020, MNRAS, 499, 4114
Gatto, M., Ripepi, V., Bellazzini, M., et al. 2021, RNAAS, 5, 159
Gatto, M., Ripepi, V., Bellazzini, M., et al. 2022a, ApJ, 931, 19
Gatto, M., Ripepi, V., Bellazzini, M., et al. 2022b, ApJL, 929, L21
Glatt, K., Gallagher, J. S. I., Grebel, E. K., et al. 2008, AJ, 135, 1106
Goodman, J., & Weare, J. 2010, Comm App Math Comp Sci, 5, 65
Górski, K. M., Hivon, E., Banday, A. J., et al. 2005, ApJ, 622, 759
Graczyk, D., Pietrzyński, G., Thompson, I. B., et al. 2020, ApJ, 904, 13
GRAVITY Collaboration, Abuter, R., Amorim, A., et al. 2019, A&A, 625,
   L10
Harris, C. R., Millman, K. J., van der Walt, S. J., et al. 2020, Natur, 585, 357
Harris, W. E. 2010, arXiv:1012.3224
Hinton, S. R. 2019, ChainConsumer: Corner Plots, LaTeX Tables and Plotting
   Walks, Astrophysics Source Code Library, ascl:1910.017
Homma, D., Chiba, M., Komiyama, Y., et al. 2019, PASJ, 71, 94
Homma, D., Chiba, M., Okamoto, S., et al. 2016, ApJ, 832, 21
Homma, D., Chiba, M., Okamoto, S., et al. 2018, PASJ, 70, S18
Jahn, E. D., Sales, L. V., Wetzel, A., et al. 2019, MNRAS, 489, 5348
Jethwa, P., Erkal, D., & Belokurov, V. 2016, MNRAS, 461, 2212
Ji, A. P., Koposov, S. E., Li, T. S., et al. 2021, ApJ, 921, 32
Kallivayalil, N., Sales, L. V., Zivick, P., et al. 2018, ApJ, 867, 19
Kim, D., & Jerjen, H. 2015a, ApJL, 808, L39
Kim, D., & Jerjen, H. 2015b, ApJ, 799, 73
Kim, D., Jerjen, H., Mackey, D., Da Costa, G. S., & Milone, A. P. 2016, ApJ,
   820, 119
Kim, D., Jerjen, H., Milone, A. P., Mackey, D., & Da Costa, G. S. 2015, ApJ,
   803.63
Koposov, S., de Jong, J. T. A., Belokurov, V., et al. 2007, ApJ, 669, 337
Koposov, S. E., Belokurov, V., Torrealba, G., & Evans, N. W. 2015, ApJ,
   805, 130
Koposov, S. E., Erkal, D., Li, T. S., et al. 2023, MNRAS, 521, 4936
Koposov, S. E., Walker, M. G., Belokurov, V., et al. 2018, MNRAS, 479, 5343
Li, T. S., Koposov, S. E., Zucker, D. B., et al. 2019, MNRAS, 490, 3508
Longeard, N., Martin, N., Ibata, R. A., et al. 2019, MNRAS, 490, 1498
Longeard, N., Martin, N., Starkenburg, E., et al. 2018, MNRAS, 480, 2609
Luque, E., Queiroz, A., Santiago, B., et al. 2016, MNRAS, 458, 603
Luque, E., Santiago, B., Pieres, A., et al. 2018, MNRAS, 478, 2006
Mackey, A. D., & Gilmore, G. F. 2004, MNRAS, 352, 153
Mackey, D., Koposov, S., Da Costa, G., et al. 2018, ApJL, 858, L21
Martin, N. F., de Jong, J. T. A., & Rix, H.-W. 2008, ApJ, 684, 1075
```

```
Martin, N. F., Jungbluth, V., Nidever, D. L., et al. 2016, ApJL, 830, L10
Martin, N. F., Nidever, D. L., Besla, G., et al. 2015, ApJL, 804, L5
Massana, P., Noël, N. E. D., Nidever, D. L., et al. 2020, MNRAS, 498, 1034
Massana, P., Ruiz-Lara, T., Noël, N. E. D., et al. 2022, MNRAS, 513, L40
Mau, S., Cerny, W., Pace, A. B., et al. 2020, ApJ, 890, 136
Mau, S., Drlica-Wagner, A., Bechtol, K., et al. 2019, ApJ, 875, 154
Mazzi, A., Girardi, L., Zaggia, S., et al. 2021, MNRAS, 508, 245
McConnachie, A. W. 2012, AJ, 144, 4
Moskowitz, A. G., & Walker, M. G. 2020, ApJ, 892, 27
Muñoz, R. R., Côté, P., Santana, F. A., et al. 2018, ApJ, 860, 66
Muñoz, R. R., Geha, M., Côté, P., et al. 2012, ApJL, 753, L15
Mutlu-Pakdil, B., Sand, D. J., Carlin, J. L., et al. 2018, ApJ, 863, 25
Nidever, D. L., Majewski, S. R., & Butler Burton, W. 2008, ApJ, 679, 432
Nidever, D. L., Olsen, K., Walker, A. R., et al. 2017, AJ, 154, 199
Pace, A. B., Erkal, D., & Li, T. S. 2022, ApJ, 940, 136
Patel, E., Kallivayalil, N., Garavito-Camargo, N., et al. 2020, ApJ, 893, 121
Piatti, A. E., & Lucchini, S. 2022, MNRAS, 515, 4005
Pieres, A., Santiago, B., Drlica-Wagner, A., et al. 2017, MNRAS, 468, 1349
Pieres, A., Santiago, B. X., Drlica-Wagner, A., et al. 2017, MNRAS, 468, 1349
Pietrzyński, G., Graczyk, D., Gieren, W., et al. 2013, Natur, 495, 76
Plummer, H. C. 1911, MNRAS, 71, 460
Richstein, H., Patel, E., Kallivayalil, N., et al. 2022, ApJ, 933, 217
Ripepi, V., Chemin, L., Molinaro, R., et al. 2022, MNRAS, 512, 563
Ripepi, V., Cignoni, M., Tosi, M., et al. 2014, MNRAS, 442, 1897
Ripepi, V., Cioni, M.-R. L., Moretti, M. I., et al. 2017, MNRAS, 472, 808
Rubele, S., Girardi, L., Kerber, L., et al. 2015, MNRAS, 449, 639
Rubele, S., Pastorelli, G., Girardi, L., et al. 2018, MNRAS, 478, 5017
Sales, L. V., Navarro, J. F., Kallivayalil, N., & Frenk, C. S. 2016, MNRAS,
Schlafly, E. F., & Finkbeiner, D. P. 2011, ApJ, 737, 103
Schlegel, D. J., Finkbeiner, D. P., & Davis, M. 1998, ApJ, 500, 525
Simon, J. D., Li, T. S., Erkal, D., et al. 2020, ApJ, 892, 137
Torrealba, G., Belokurov, V., Koposov, S. E., et al. 2018, MNRAS, 475, 5085
Torrealba, G., Belokurov, V., & Koposov, S. E. 2019, MNRAS, 484, 2181
Torrealba, G., Koposov, S. E., Belokurov, V., et al. 2016a, MNRAS, 463, 712
Torrealba, G., Koposov, S. E., Belokurov, V., & Irwin, M. 2016b, MNRAS,
  459, 2370
van der Marel, R. P., & Kallivayalil, N. 2014, ApJ, 781, 121
van der Walt, S., Colbert, S. C., & Varoquaux, G. 2011, CSE, 13, 22
Virtanen, P., Gommers, R., Oliphant, T. E., et al. 2020, NatMe, 17, 261
Wang, M. Y., de Boer, T., Pieres, A., et al. 2019, ApJ, 881, 118
Weisz, D. R., Koposov, S. E., Dolphin, A. E., et al. 2016, ApJ, 822, 32
Zonca, A., Singer, L., Lenz, D., et al. 2019, JOSS, 4, 1298
```